A Wide Frequency Range Surface Integral Formulation for 3-D RLC Extraction

J. Wang*, J. Tausch** and J. White*

* Department of Electrical Engineering and Computer Science, M.I.T. Cambridge, MA. 02139
** Southern Methodist University, tausch@golem.math.smu.edu

Abstract

A new surface integral formulation and discretization approach for computing electromagnetoquasistatic impedance of general conductors is described. The key advantages of the formulation is that it avoids volume discretization of the conductors and the substrate, and a single discretization is accurate over the entire frequency range. Computational results from an on-chip inductor, a connector and a transmission line are used to show that the formulation is accurate and is "acceleration" ready. That is, the results demonstrate that an efficiently computed preconditioner insures rapid iterative method convergence and tests with projection show the required kernels can be approximated easily using a coarse grid.

Keywords: Electromagnetics, Impedance extraction, Surface integral equation, PEEC, FastHenry,

1 Introduction

In this paper we describe a surface integral formulation and discretization approach to computing electromagnetoquasistatic impedance of general conductors. The key advantages of this formulation is that it avoids volume discretization of the conductors and the substrate, and a single discretization is accurate over the entire frequency range. In addition, the approach does not require a-priori information about surface impedances, does not include assumptions about proximity effects, and does not switch to volume formulations at low frequencies [3], [2], [1]. In the next section the integral formulation is derived, and in section 3 the discretization is presented. In section 4, we present results for a spiral inductor, a connector and a tranmission line and compare to the publicly available FastHenry program and analytic formulas. In section 5 we show that the discretized system can be efficiently solved iteratively and that the kernels involved can be projected onto a coarse grid. We present the data in section 5 to demonstrate that even though we have not yet completed a fast solver for the approach, the formulation is suitable for acceleration.

1.1 Surface Integral Formulation

In the interior of any conductor, the electric field, denoted $\bar{E}$, satisfies

$$\nabla^2 \bar{E} - i\omega\mu\sigma\bar{E} = 0 \quad or \quad \nabla^2 \bar{E} = i\omega\mu\bar{J}. \tag{1}$$

where σ is the conductor conductivity, μ is the permeability, and $\bar{J}$ is the current density. Applying Green's Theorem to the left-hand equation in (1) yields a dyadic surface integral equation

$$\int_{S_m} G_1(x,y)\frac{\partial \bar{E}(y)}{\partial n_y}dy - \int_{S_m}\frac{\partial G_1(x,y)}{\partial n_y}\bar{E}(y)dy = \bar{E}(x) \tag{2}$$

where S_m is the surface of the mth conductor,

$$G_1(x,y) = \frac{e^{ik_1|x-y|}}{4\pi|x-y|},\ k_1 = \sqrt{-i\omega\mu\sigma} \tag{3}$$

and x and y are on S_m. Note that we use the simpler notation in which $\int_S \frac{\partial G_1(x,y)}{\partial n_y}\bar{E}(y)dy$ is the entire integral rather than decomposing the integral into an extra term and a principle-value integral.

A similar-looking dyadic integral equation can be derived by applying Green's Theorem to the right-hand equation in (1) and then eliminating $\bar{J}$ using the relation $-\nabla\psi = \bar{E} + i\omega\int_V \mu G_0(x,y)\bar{J}(y)dy$. The result is

$$\int_S G_0(x,y)\frac{\partial \bar{E}(y)}{\partial n_y}dy - \int_S \frac{\partial G_0(x,y)}{\partial n_y}\bar{E}(y)dy + \nabla\psi(x) = 0 \tag{4}$$

where S is the union of conductor surfaces, and

$$G_0(x,y) = \frac{1}{4\pi|x-y|} \tag{5}$$

The scalar potential ψ satisfies the Poisson equation, and since the only nonzero charge in the problem is on the conductor surfaces, the scalar potential is given by

$$\int_S G_0(x,y)\rho_s(y)dy = \epsilon\psi(x), x, y \in S \tag{6}$$

where ρ_s denotes the surface charge density.

The equations derived above are three sets of equations for four sets of variables, E, $\frac{\partial E}{\partial n}$, ψ and ρ_s. The needed additional equation can be derived by enforcing current conservation. Since there is no interior charge, current conservation implies $\nabla \bullet E = 0$ in the conductor interiors.

2 Discretization

In order to solve the system of integral equations, (2), (4) and (6), consider discretizing the surface into N quadrilateral panels. In such a discretization, a quadrilateral panel vertex will be shared by four panels. We associate 7 unknowns with each panel: $\frac{\partial E_x}{\partial n}$, $\frac{\partial E_y}{\partial n}$, $\frac{\partial E_z}{\partial n}$, E_x, E_y,E_z and q. The scalar potential is associated with the panel vertices.

The panel unknowns are assumed to be constant over a panel. Then, if centroid collocation is used to solve (2) the result is a $3N \times 6N$ system

$$P_1 \frac{\partial \bar{E}}{\partial n} - (D_1 + \frac{1}{2} I)\bar{E} = 0 \tag{7}$$

where

$$\begin{aligned} P_1(i,j) &= \int_{panel_j} G_1(x_i, y)dy \\ D_1(i,j) &= \int_{panel_j} \frac{\partial G_1}{\partial n_y}(x_i, y)dy \end{aligned}$$

and x_i is the i^{th} collocation point.

Collocation applied to (4) will result in an equation similar in form to (7), but will include a $\nabla\psi$ term. The $\nabla\psi$ term is difficult to compute as the surface-normal derivative of the potential can not be evaluated using only the vertex potentials. Instead, consider applying collocation to (4) but extracting out only the surface tangential components as in

$$TP_0 \frac{\partial \bar{E}}{\partial n} - TD_0\bar{E} + A_t\psi = 0 \tag{8}$$

where T is the $2N \times 3N$ matrix which extracts the tangential components at the panel centroids,

$$\begin{aligned} P_0(i,j) &= \int_{panel_j} G_0(x_i, y)dy \\ D_0(i,j) &= \int_{panel_j} \frac{\partial G_0}{\partial n_y}(x_i, y)dy \end{aligned}$$

and A_t is the operator that computes the surface tangential components of $\nabla\psi$ using finite-differences on the vertex potentials. In order to replace the missing normal direction equation, one can use the fact that

$$n \bullet \bar{E} = \frac{i\omega\rho_s}{\sigma}. \tag{9}$$

where ρ_s is the vector of panel charge densities.

The charge on a panel can be related to the weighted average of the panel's vertex potentials, as in

$$P_0\rho_s = \epsilon A\psi \tag{10}$$

where A is the matrix of potential averaging coefficients.

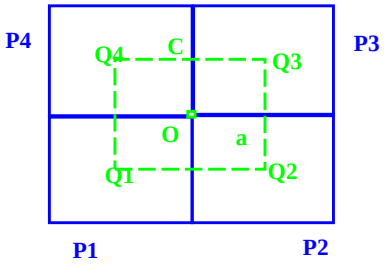

Figure 1: Dual panel for current conservation

Equations (7), (8), (9) and (10) represents seven equations for each panel, matching the seven panel electric field and charge unknowns. In order to generate a set of equations for the vertex potentials, consider applying current conservation to dual panels, as shown in Figure 1. Node O in the figure is the vertex at the corner of four panels. The dual panel is denoted by the dashed line that connects four panel centroids.

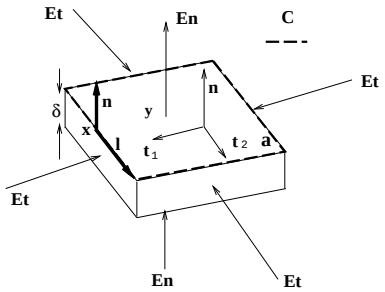

Figure 2: A thin box just under the conductor surface.

Now consider a thin box just underneath the dual panel as shown in Figure 2. Letting the thickness of the box approach zero results in an integral relation

$$\int_C E_t(x) \bullet (n(x) \times l(x))dx - \int_a \frac{\partial E_n(y)}{\partial n(y)}dy = 0. \tag{11}$$

By examining Figure 2, it is clear that $E_t(x)$ and $\frac{\partial E_n(y)}{\partial n(y)}$ in (11) can be approximated by averaging the surrounding panel field and field derivatives.

3 Numerical Accuracy Experiments

In this section we present results from using the above formulation to perform both magnetoquasistatic and electromagnetoquasistatic analysis of several structures. We start by performing magnetoquasistatic analysis of a multipin connector and a spiral inductor over a semiconductor substrate ground plane, and compare the results to the public domain program FASTHENRY [4]. We then perform electromagnetoquasistatic analysis of a transmission line, and compare the results to an analytic formula.

3.1 Multipin Connector

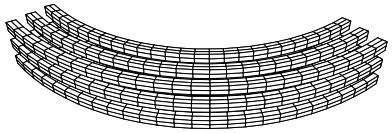

Figure 3: A 3 by 3 curved connector example

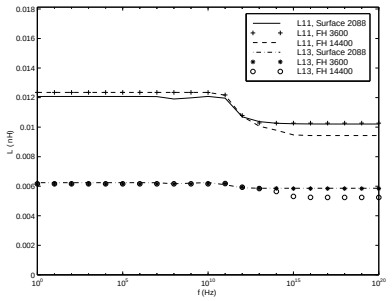

Figure 4: Inductance for a 3 by 3 curved connector

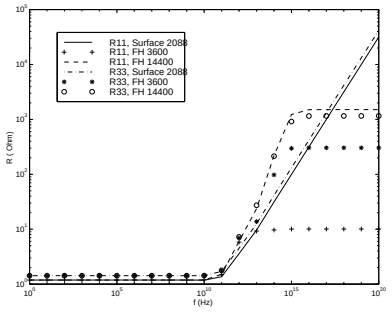

Figure 5: Resistance for a 3 by 3 curved connector

Our surface formulation was used to compute the frequency-dependent magnetoquasistatic inductance (Fig. (4)) and resistance (Fig. (5)) of the curved multipin connector shown in Fig. (3). The plots show three sets of computations, one with our surface formulation using 2088 panels, one using FASTHENRY (denoted FH) with 3600 filaments, and one using FASTHENRY with 14400 filaments. As the resistance plots show, the surface formulation captures the correct frequency dependence of the resistance, but the FASTHENRY results are only accurate to a discretization dependent frequency. There are a few anomalies in the plots generated by FASTHENRY for the fine discretization due to a well-known problem with FASTHENRY's filament integrals [6].

3.2 Spiral Inductor

The second example(Figure 6) is a spiral inductor with and without a semiconductor substrate ground plane. The diameter of the spiral is about 100um, with a 5um by 5um cross section. The ground plane is about 400um by 400um, and is 100um thick. The conductivity of the spiral is that of copper, and the conductivity of the ground is .005 that of copper.

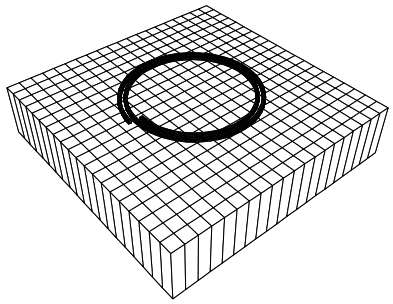

Figure 6: A spiral inductor over a substrate ground plane

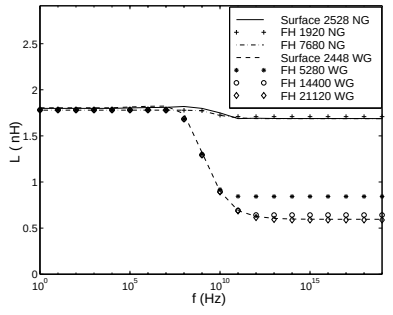

Figure 7: Inductance for the spiral inductor with and without a substrate ground plane

The simulation results show the same trends as the first example. As shown in Fig. (7), the surface for-

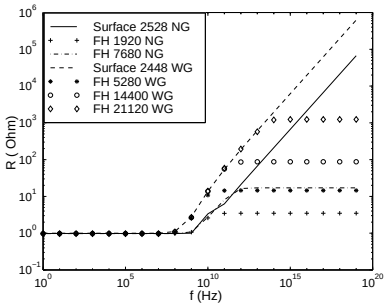

Figure 8: Resistance for the spiral inductor with and without a substrate ground plane

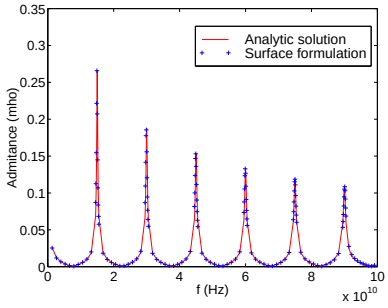

Figure 9: Admittance of the long transmission line

mulation matches the inductance computed by FASTHENRY over the entire frequency range. Both methods capture the drop of inductance due to skin and proximity effects. Again, the surface formulation correctly captures the frequency-dependent resistance over the entire frequency range, but FASTHENRY does not, as shown in Figure 8. One final note, it was necessary to use more than 21,000 filaments in the substrate ground plane to converge the FASTHENRY results, where only 2500 panels were needed in the surface formulation.

3.3 Transmission Line

To verify that the surface formulation can perform EMQS analysis, the admittance of a long shorted transmission line was computed and then compared to the analytic formula for a 2-D shorted transmission line. The transmission line wires were 37 microns wide, 15 microns thick and 10000 microns long. The two lines were seperated by a gap of 27 microns. To compute the admittance using the surface formulation, the two wires of the transmission line were discretized into a total of 804 panels. To compute the admittance using 2-D analysis, an effective inductance and capacitance per unit length were computed numerically. The results are compared in Fig. (9), and clearly show that the surface formulation correctly captures the resonances.

4 Fast Solution Algorithms

The surface formulation and discretization described above generates $3N \times 3N$ and $2N \times 3N$ dense block matrices, and so can not be used directly to analyze complicated structures. Instead, the integral formulation must be combined with an accelerated iterative method which allows for general Green's functions, such as the Precorrected-FFT algorithm [5] or the hierarchal SVD [7] approach. Although we have not yet implemented an accelerated version of our formulation, in this section we try to demonstrate that acceleration will be effective. In particular, we demonstrate that we have a preconditioner which insures rapid Krylov-subspace method convergence and that the $\frac{e^{ik_1|x-y|}}{4\pi|x-y|}$ kernel can be well approximated using the Precorrected-FFT grid.

The preconditioner used directly factors a system made up of the sparse blocks, as well as the diagonals of the dense blocks, in (7), (8), (9), (10) and (11). The preconditioner was combined with GMRES and used to solve all the examples in the previous section, over the entire frequency range. The results are tabulated in Table (1). As is clear from the table, the iterative always converges in fewer than 100 iterations.

Problem	panel	unknown	Min iter	Max iter
connector	2088	14850	16	41
spiral NG	2528	17704	5	67
spiral WG	2448	17184	27	81
tranmission	804	6452	4	10

Table 1: Size of the problem and GMRES iteration number

The only kernel that has not been previously accelerated with the Precorrected-FFT algorithm is the $\frac{e^{ik_1 r}}{r}$ kernel, as here k_1 is imaginary. To show the Precorrected-FFT algorithm will have no difficulty with this kernel, we projected a point source onto vertex sources of a 2 by 2 by 2 cube. In Figure 10, the worst case error at a distance of 3 from the cube center is plotted as a function of frequency. This plot shows that even for this low order projection, the error is never worse than a few percent.

5 Conclusions and Acknowledgements

In this paper we described a surface integral formulation and discretization approach to computing electromagnetoquasistatic impedance of general conductors.

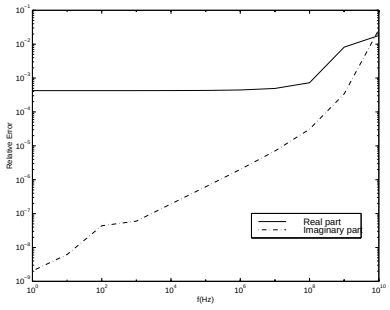

Figure 10: Worst case projection error for a typical example

The key advantages of this formulation is that it avoids volume discretization of the conductors and the substrate, and a single discretization is accurate over the entire frequency range. We showed by examining a spiral inductor, a connector and a transmission line example that the formulation is accurate and "acceleration ready". We are currently working on implementing a version of the approach which uses the Precorrected-FFT accelerated algorithm.

The authors would like to acknowledge support from the DARPA MURI program and the DARPA composite-CAD program. In addition, this work was also supported by the Semiconductor Research Corporation and Grants from Hewlett-Packard.

REFERENCES

[1] E. Tuncer, Beom-Taek Lee, and D. P. Neikirk, "Interconnect Series Impedance Determination Using a Surface Ribbon Method" IEEE 3rd Topical Meeting on Electrical Performance of Electronic Packaging, Monterey, CA, Nov. 2-4, 1994, pp. 250-252.

[2] R.B. Wu and J.C. Yang,"Boundary integral equation formulation of skin effect problem in multiconductor transmission lines" IEEE Trans. Magnetics, vol. Mag-25, pp.3013-3015, July 1989.

[3] M.J. Tsuk and J.A.Kong, "A Hybrid Method for the calculation of the resistance and inductance of transmission lines with arbitrary cross sections" Microelectronic System Interconnections, pp65-pp74.

[4] M. Kamon M.J. Tsuk and J.K. White," FASTHENRY: A multipole accelerated 3-D Inductance Extraction Program", IEEE Trans. MTT, vol.42., No.9, pp1750–pp1758, Sep.1994.

[5] J. R. Phillips and J. K. White, "A Precorrected-FFT method for Electrostatic Analysis of Complicated 3-D Structures," *IEEE Trans. on Computer-Aided Design*, October 1997, Vol. 16, No. 10, pp. 1059-1072.

[6] M. Kamon, F. Wang and J. White, "Recent Improvements to Fast Inductance Extraction and Simulation," Proceedings of the 7^{th} Topical Meeting on Electrical Performance of Electronic Packaging West Point, New York, October, 1998, pp. 281-284

[7] S. Kapur and J. Zhao,"A fast method of moments solver for efficient parameter extraction of MCMs" Design Automation Conference, 1997 pp. 141–146.